

	SAKARYA UNIVERSITY JOURNAL OF SCIENCE		 SAKARYA UNIVERSITY
	e-ISSN: 2147-835X http://www.saujs.sakarya.edu.tr		
	<u>Received</u> 02-01-2018 <u>Accepted</u> 10-05-2018	<u>Doi</u> 10.16984/saufenbilder.373607	

Preparation and antibacterial activity of solvothermal synthesized ZnFe₂O₄/Ag-TiO₂ nanocomposite

Keziban Atacan^{*1}, Nuray Güy², Soner Çakar³

Abstract

In this study, ZnFe₂O₄ magnetic nanoparticles and ZnFe₂O₄/Ag-TiO₂ nanocomposite were synthesized solvothermally. The prepared materials were characterized using X-ray diffraction, Scanning electron microscopy, Fourier transform infrared spectroscopy and Vibrating sample magnetometer. In addition, the antibacterial performance of materials was evaluated against Gram-positive bacteria (*Staphylococcus aureus*) and Gram-negative bacteria (*Escherichia coli*). ZnFe₂O₄/Ag-TiO₂ nanocomposite was shown more powerful antibacterial efficiency against *Staphylococcus aureus* than *Escherichia coli*. Also, the inhibition diameter of 15±0.2 mm for ZnFe₂O₄/Ag-TiO₂ nanocomposite was measured since the antibacterial activity increased with nanocomposite formation.

Keywords: ZnFe₂O₄, TiO₂, silver nanoparticles, antibacterial activity

1. INTRODUCTION

Spinel ferrites have been extensively investigated in recent years in various fields, such as biomedical fields, optoelectronic devices, catalysis and drug loading materials owing to their physical, chemical and magnetic properties [1]. Furthermore, spinel ferrites have major features for many fields, including the elimination of contaminants from water and air, odor control, bacterial inactivation, water splitting for H₂ production, and many others [2]. Among various spinel ferrites, zinc ferrite (ZnFe₂O₄) magnetic nanoparticles (MNPs) have been widely used both drug delivery systems and other biomedical, biotechnology applications. ZnFe₂O₄ is synthesized by using various

techniques including sol-gel, coprecipitation and hydrothermal/solvothermal method and so on [3, 4]. Among them, the solvothermal synthesis is easy to control morphology of the products, so it is generally preferred [4, 5].

The substitution of spinel ferrite with a transition metal can increase the antibacterial property of ferrite nanoparticles (NPs) in biomedical applications. The spinel ferrite NPs have been required further study for biomedical application due to their biocompatibility and antibacterial properties [6, 7]. The modification of NPs with noble metals, such as Pt, Au, and Pd, has been accepted as one of the most efficient methods to improve the stability, biocompatibility and bacterial activity for biological applications [8]. Besides the other metal (Au, Ag, Cu, Pt, Pd, etc.)

*Corresponding Author: kezibanatacan@sakarya.edu.tr

¹Sakarya University, Biomedical, Magnetic and Semiconductor Materials Research Center (BIMAS-RC), 54187 Sakarya, Turkey

²Sakarya University, Science & Arts Faculty, Department of Chemistry, 54187 Sakarya, Turkey

³Bulent Ecevit University, Science and Technology Research and Application Center (ARTMER), 67100 Zonguldak, Turkey

NPs, the silver NPs (Ag NPs) have a lot of interest due to their low-cost and stability, large specific surface area and excellent antimicrobial activities [9]. Ag NPs have long been known to exert strong inhibitory and bactericidal effects. The Ag NPs with their unique chemical and physical properties are noted for an alternative for improving of new antibacterial materials due to their antimicrobial properties. The NPs get adhered to the bacterial membrane and also some of them pass through inside of the cell membrane. The bacterial membrane includes sulfur-containing proteins and so the Ag NPs are interacted with these proteins in the cell [10]. Furthermore, Ag NPs have widely used for various fields such as food, package and medicine due to having high surface area and physicochemical properties [11]. To the best of our knowledge, TiO₂ NPs have been found to be effective as antibacterial agent against both Gram-positive and Gram-negative bacteria. Verma et al. stated that TiO₂ NPs have their efficiency against the bacterial biofilm formed by *Enterobacter sp.* [12]. Chan et al. studied antibacterial activity of TiO₂ nanotubes against Gram-positive bacteria (*Bacillus atrophaeus*) as a function of annealing temperature [13].

Although some papers on antibacterial activities of TiO₂ and Ag-TiO₂ derivatives have been published, there have been no investigation on the antibacterial activity of ZnFe₂O₄/Ag-TiO₂ nanocomposite [14, 15]. The goal of this study is to investigate preparation, characterization and the antibacterial properties of ZnFe₂O₄/Ag-TiO₂ nanocomposite.

2. MATERIALS AND METHODS

2.1. Materials

All chemicals were of analytic grade and used as received without further purification. ZnCl₂ (>99%), FeCl₃.6H₂O (>99%), CH₃COONa.3H₂O (NaAc, >99%), NaOH (≥97%), NaBH₄ (≥96%), C₂H₅OH (>99.2%), Chromocult Coliform Agar and Baird Parker Agar were provided from Merck (Germany). Titanium isopropoxide (TTIP, 97%) was obtained from Sigma-Aldrich (USA). C₂H₆O₂ (99%, EG) and AgNO₃ were provided from Tekkim (Turkey).

2.2. Preparation of ZnFe₂O₄, TiO₂, Ag-TiO₂ and ZnFe₂O₄/Ag-TiO₂ nanocomposite

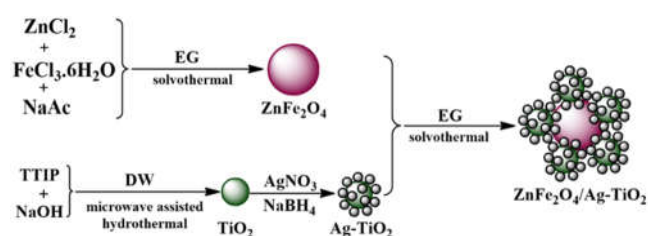
ZnFe₂O₄ magnetic NPs were synthesized through a solvothermal method with minor modifications [4, 16]. 0.34 g ZnCl₂ (1 mmol), 1.08 g FeCl₃.6H₂O (2 mmol) and 0.82 g of NaAc (4 mmol) were dissolved into 30 mL of EG under vigorous stirring for 1 h at room temperature. Then, the homogeneous solution was transferred into Teflon-coated autoclave (40 mL) and held at 180 °C for 18 h in furnace. The autoclave was cool. Finally, ZnFe₂O₄ MNPs were collected by a magnet and then they were washed with deionized water (DW) several times, washed with ethanol and dried at 70 °C for 24 h.

TiO₂ NPs were prepared by using microwave assisted hydrothermal method with some modification [17]. TTIP (5 mL) and 1 M NaOH (5 mL) were dissolved in DW (60 mL). After stirring intensively for 1 h at room temperature, the mixture was transferred into the Teflon-coated autoclave microwave assisted hydrothermal vessel and conducted microwave irradiation (CEM Mars5 model) with a controlled power of 380 W for 30 min at 100 °C. TiO₂ NPs were centrifuged at 5000 rpm for 15 min and washed with DW several times and ethanol. Then the obtained white powder was dried at 70 °C for 24 h.

For the doped Ag on TiO₂, 0.5 g of TiO₂ were dispersed in 40 mL of DW under ultrasonication for 30 min. After AgNO₃ was added to this reaction such that the gravimetric weight ratio of Ag to TiO₂ reaction was 5% [18], 0.0175 M (20 mL) NaBH₄ solution was added drop by drop to the mixture and stirred for 1 h. So, silver ions (Ag⁺) were reduced and clustered to metallic NPs (Ag) onto TiO₂ surface. The Ag-TiO₂ particles were centrifuged and washed twice with DW and ethanol. Then, the Ag-TiO₂ was dried at 70 °C for 24 h.

For the preparation of ZnFe₂O₄/Ag-TiO₂ nanocomposite, 0.035 g ZnFe₂O₄ MNPs and 0.07 g Ag-TiO₂ were dispersed into 30 mL of EG under vigorous stirring at room temperature for 30 min. Then, the mixture was transferred into Teflon-coated autoclave and heated at 180 °C for 4 h [19]. The autoclave was allowed to cool. ZnFe₂O₄/Ag-TiO₂ nanocomposite (mass ratio=2:1) was collected by a magnet. The separation, washing and drying process were carried out according to the same as ZnFe₂O₄ MNPs. Preparation of

ZnFe₂O₄/Ag-TiO₂ nanocomposite was shown in Scheme 1.



Scheme 1. Preparation of ZnFe₂O₄/Ag-TiO₂ nanocomposite

2.3. Test of antibacterial activity

The antibacterial activities of ZnFe₂O₄, TiO₂, Ag-TiO₂ and ZnFe₂O₄/Ag-TiO₂ were tested against the Gram-negative bacterium *Escherichia coli* (*E. coli*) and the Gram-positive bacterium *Staphylococcus aureus* (*S. aureus*). *E. coli* and *S. aureus* were grown aerobically at 37 °C overnight. 1 mL of fresh bacterial suspension was prepared from *E. coli* and *S. aureus* bacteria at room temperature using physiological saline solution and vortexed. After 0.1 mL aliquot of bacterial suspension was poured on sterile Petri dishes on the Chromocult Coliform Agar plate for *E. coli* and on the Baird Parker Agar plate for *S. aureus*. All samples were put in stated agar plate. Finally, petri dishes were incubated at 37 °C for 24 h in the dark [20]. After 24 h, all petri dishes were visually controlled for the presence of bacterial growth, and the zone of inhibition (ZOI) was measured. The test was performed in triplicate.

2.4. Characterizations of all samples

The prepared products were confirmed by XRD (PANalytical, Empyrean, Netherlands). FTIR spectra were recorded on Shimadzu UATR Two instrument (Japan). The morphologies of the samples were characterized using a Philips XL30 SFEG scanning electron microscope (SEM). Magnetic measurements were recorded at 300 K using vibration sample magnetometry (VSM Lake Shore-7407, USA).

3. RESULTS AND DISCUSSION

3.1. X-ray diffraction

Figure 1 shows the XRD patterns of ZnFe₂O₄, TiO₂, Ag-TiO₂ and ZnFe₂O₄/Ag-TiO₂. The XRD pattern of the pure ZnFe₂O₄ in Figure 1 can be perfectly assigned to the cubic phase of ZnFe₂O₄ (ICSD no. 98-009-1931). The diffraction peaks at $2\theta = 30.13^\circ$, 35.48° , 43.14° , 53.55° , 57.02° , and

62.67° were indexed to the (220), (311), (400), (422), (511) and (440) reflections of ZnFe₂O₄ with cubic spinel structure [19, 21]. The XRD spectra of TiO₂ indicated anatase phase formation (ICDS: 98-015-4601) due to (101) crystal plane [17]. As shown in Figure 1, the six diffractive peaks at 25.28° , 37.95° , 47.98° , 53.84° , 54.88° and 62.72° can be indexed to the (101), (004), (200), (105), (211), and (204) crystal planes of anatase TiO₂, respectively [8, 22]. The XRD pattern of Ag-TiO₂ shows the characteristic peaks corresponding to anatase TiO₂ phase. However, no diffraction peaks of Ag phase are observed, which confirms that the Ag particles are very small and dispersed on the TiO₂ support [14]. The invisibly diffraction peaks for Ag-TiO₂ at 37.88° and 44.50° reflect the crystallographic planes of (111) and (200) for the face-centered cubic of the silver crystal in Figure 1 [11]. At the XRD pattern of ZnFe₂O₄/Ag-TiO₂ nanocomposite, it can be seen that all added peaks are in good agreement with both ZnFe₂O₄ and Ag-TiO₂. In addition, no peaks related to other impurities are observed in the synthesized ZnFe₂O₄/Ag-TiO₂ nanocomposite, indicating that no chemical reaction between ZnFe₂O₄ and Ag-TiO₂ occurs.

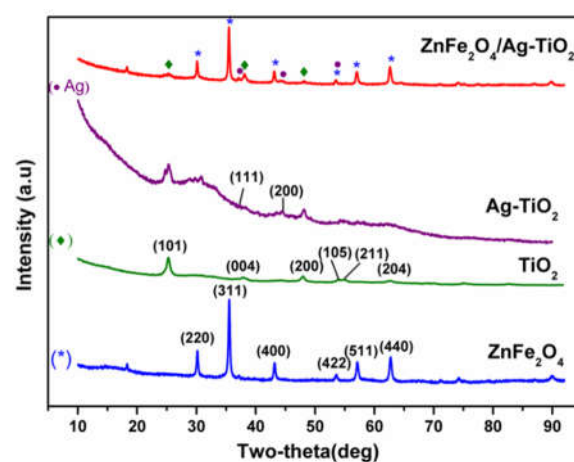


Figure 1. XRD patterns of ZnFe₂O₄, TiO₂, Ag-TiO₂ and ZnFe₂O₄/Ag-TiO₂

3.2. Fourier transform infrared spectroscopy

FTIR spectra of ZnFe₂O₄, TiO₂, Ag-TiO₂ and ZnFe₂O₄/Ag-TiO₂ indicated in Figure 2 in the range of 400–4000 cm⁻¹. From the FTIR spectrum of ZnFe₂O₄ MNPs, the strong and sharp absorption band appeared at 540 cm⁻¹ is in good agreement with vibration of Fe–O as typical band of spinel ferrite [23]. In addition, it can be found that the stretching vibration of Zn–O appears at 430 cm⁻¹, which corresponds to the M–O of the octahedron in the spinel structure [24]. According to Figure 2, a broad band below 1000 cm⁻¹ was monitored at

the spectra of both TiO_2 and Ag-TiO_2 , which can be assigned to the bending and stretching vibrations of Ti-O-Ti bonds [22]. In the FTIR of $\text{ZnFe}_2\text{O}_4/\text{Ag-TiO}_2$, most of the oxygen containing functional groups have been weakened during the solvothermal process [25]. However, the two characteristic absorption peaks of ZnFe_2O_4 exhibit slight shift in the curve of $\text{ZnFe}_2\text{O}_4/\text{Ag-TiO}_2$ nanocomposite (Figure 2), which also suggests that there are some interactions between ZnFe_2O_4 and Ag-TiO_2 in $\text{ZnFe}_2\text{O}_4/\text{Ag-TiO}_2$ nanocomposite.

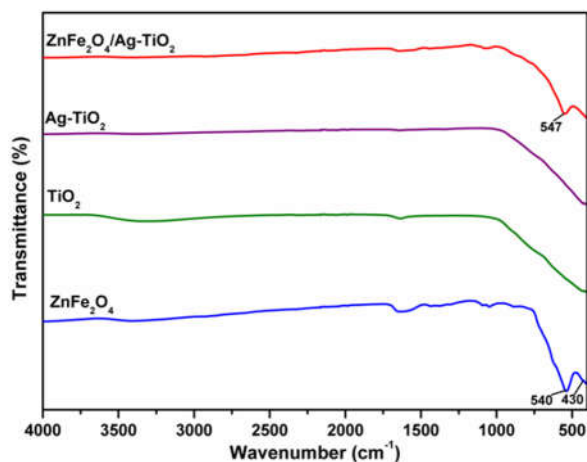


Figure 2. FTIR spectra of ZnFe_2O_4 , TiO_2 , Ag-TiO_2 and $\text{ZnFe}_2\text{O}_4/\text{Ag-TiO}_2$

3.3. Magnetic measurements

The magnetic properties of all samples were investigated by vibrating sample magnetometer (VSM) at room temperature, and the magnetic hysteresis loops are depicted in Figure 3. The saturation magnetization values of ZnFe_2O_4 MNPs is 12 emu/g. ZnFe_2O_4 MNPs are also superparamagnetic, as its magnetic hysteresis loop passed through the origin of the coordinate [19]. For TiO_2 and Ag-TiO_2 , the saturation magnetization values of 1.1 and 2.4 emu/g were obtained respectively. The $\text{ZnFe}_2\text{O}_4/\text{Ag-TiO}_2$ nanocomposite exhibits the saturation magnetization of 5.5 emu/g. The saturation magnetization of the magnetic composite decreases compared with that of ZnFe_2O_4 MNPs, which can be attributed to the less magnetic source.

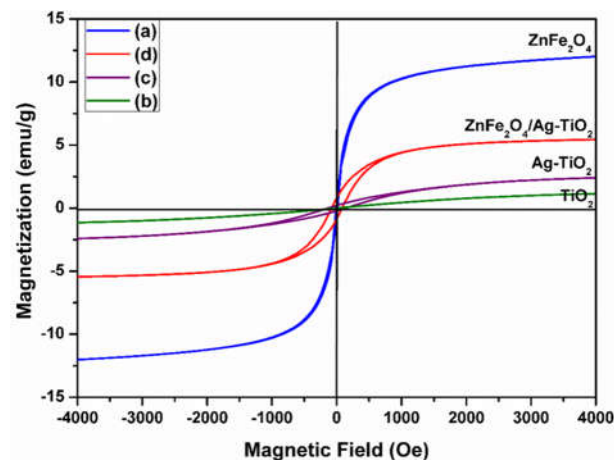


Figure 3. Magnetization hysteresis loops of ZnFe_2O_4 (a), TiO_2 (b), Ag-TiO_2 (c) and $\text{ZnFe}_2\text{O}_4/\text{Ag-TiO}_2$ (d)

3.4. Scanning Electron Microscopy

The morphology of all samples were investigated by scanning electron microscope, as shown in Figure 4. ZnFe_2O_4 MNPs are agglomerated NPs and their images show clustered structures and cauliflower-like shapes in Figure 4 (a). The TiO_2 shows very regular rough spherical morphology in Figure 4 (b). When silver NPs were doped, the size of TiO_2 decreased and no regular spherical particles was obtained in Figure 4 (c). The SEM image of the Ag-TiO_2 , confirmed that the Ag-TiO_2 distributed as reunite state and the aggregated particle [26]. As seen in Figure 4 (d), the agglomerated structure happens the scattered, which implies the $\text{ZnFe}_2\text{O}_4/\text{Ag-TiO}_2$ nanocomposite consisting of ZnFe_2O_4 and Ag-TiO_2 .

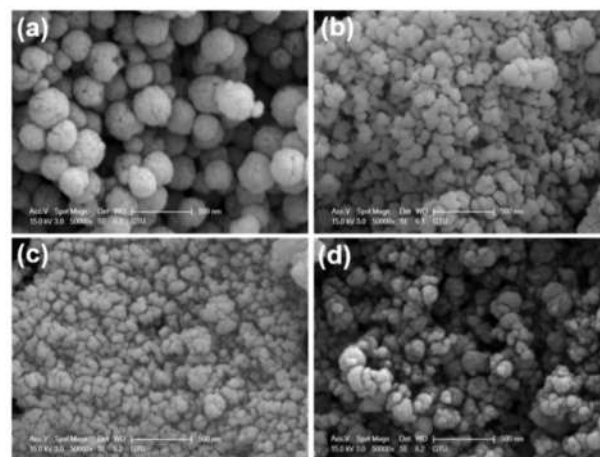


Figure 4. SEM images of ZnFe_2O_4 (a), TiO_2 (b), Ag-TiO_2 (c) and $\text{ZnFe}_2\text{O}_4/\text{Ag-TiO}_2$ (d)

3.5. Antibacterial activities of all samples

The antibacterial activities and the diameter for ZOI of the all samples against *S. Aureus* (gram-positive) and *E. coli* (gram-negative) were measured (Table 1). All samples showed stronger

antibacterial properties against *S. aureus* than *E. coli*. Gram-positive and gram-negative bacteria have differences in their membrane structure, the most distinctive of which is the thickness of the peptidoglycan layer. The peptidoglycan layer is a specific membrane feature of bacterial species. Therefore, the antibacterial effect of samples are associated with the peptidoglycan layer [27]. So, the maximum antibacterial activity was observed against *S. aureus* showing 15 mm but *E. coli* showed 12 mm (Table 1). It can be seen that, all materials have larger inhibition zone, indicating that the materials with antibacterial activities [28].

Zinc ferrite NPs can increase both their bioactivity and bactericidal efficiency owing to a large surface-to-volume ratio. As a result, the diameter of ZOI for ZnFe_2O_4 is 11 mm against *S. Aureus* but the diameter of ZOI for ZnFe_2O_4 is 8 mm against *E. coli* (Table 1). Sanpo et al. stated the antibacterial activity of transition zinc-substituted cobalt ferrite NPs ($\text{Co}_{0.5}\text{Zn}_{0.5}\text{Fe}_2\text{O}_4$) was assayed against *E. coli*. Then, they have confirmed that antibacterial activity is stronger against *E. coli* than nickel-substituted cobalt ferrite NPs ($\text{Co}_{0.5}\text{Ni}_{0.5}\text{Fe}_2\text{O}_4$) and manganese-substituted cobalt ferrite NPs ($\text{Co}_{0.5}\text{Mn}_{0.5}\text{Fe}_2\text{O}_4$) [7]. This could be based on the difference in chemical composition and surface roughness of the NPs. Also, Sanpo et al. reported that zinc-substituted cobalt ferrite nanopowders inhibit the growth of both *E. coli* and *S. aureus* [6].

TiO_2 displays good antimicrobial activity against *S. aureus* than *E. coli* (Table 1). In addition, the diameter of the ZOI for Ag-TiO_2 is larger than that of pure TiO_2 . Ag NPs decorated in nano TiO_2 are one of the methods that can improve antibacterial activity [29]. Ag NPs considerably decrease bacterial infections due to have high surface areas and so Ag NPs exhibit better antibacterial activities than the other nanoparticles. So, Ag NPs can reach more simply into the bacteria, causing mutilation on the respiration of bacteria and finally inducing to death of bacterial cell [20]. Reducing the particle size of the materials, the materials are more developed as biocompatibility and bacterial activity. Cao et al. synthesized Ag/TiO_2 and Ag/TiO_2 nanopowder by SEA method and they proved both of the antibacterial samples to be great inhibitory efficiency of mould growth in attacking and destructing bacterial cell membranes [14].

The $\text{ZnFe}_2\text{O}_4/\text{Ag-TiO}_2$ nanocomposite displays antibacterial activity against both *S. aureus* and *E. coli*, also the ZOI for $\text{ZnFe}_2\text{O}_4/\text{Ag-TiO}_2$ is larger

than that of ZnFe_2O_4 and Ag-TiO_2 (Table 1). Allafchian et al. synthesized $\text{NiFe}_2\text{O}_4/\text{PAMA}/\text{Ag-TiO}_2$ nanocomposite and they found that $\text{NiFe}_2\text{O}_4/\text{PAMA}/\text{Ag-TiO}_2$ nanocomposite showed a very good antibacterial activity against gram positive and negative bacteria [29]. Atacan et al. investigated antibacterial activities of $\text{Ag}/\text{CuFe}_2\text{O}_4$ and papain immobilized $\text{Ag}/\text{CuFe}_2\text{O}_4$ MNPs. They have found that papain immobilized $\text{Ag}/\text{CuFe}_2\text{O}_4$ MNPs show strong antibacterial efficiency [30]. This paper exhibits that after composing of nanocomposite, the antibacterial activity is significantly enhanced. The obtained results were conformed with the antibacterial properties and inhibition diameters when compared with other literatures.

Table 1. The diameters of zones of inhibition for all prepared samples in this study

Samples	ZOI (mm)	
	<i>S. Aureus</i>	<i>E. Coli</i>
ZnFe_2O_4	11±0.2	8±0.3
TiO_2	8±0.2	5±0.4
Ag-TiO_2	10±0.3	7±0.3
$\text{ZnFe}_2\text{O}_4/\text{Ag-TiO}_2$	15±0.2	12±0.3

4. CONCLUSIONS

In this study, we synthesized solvothermally $\text{ZnFe}_2\text{O}_4/\text{Ag-TiO}_2$ which exhibit antibacterial activity against *E. coli* and *S. aureus* bacteria. The main property of ZnFe_2O_4 MNPs can supply easier separation of NPs by using external magnetic field to avoid time consuming centrifugation in potential applications. By the way, the results indicated that all synthesized samples have stronger antibacterial activities against *S. aureus* than *E. coli* bacteria. But, the results indicated that the $\text{ZnFe}_2\text{O}_4/\text{Ag-TiO}_2$ nanocomposite have the most effective antibacterial property against *S. aureus* bacteria among all of the samples investigated in this study. The magnetic nanocomposite was proved to have both the good antibacterial activity of Ag-TiO_2 and the ZnFe_2O_4 MNPs. So, this work demonstrates that after composing of nanocomposite formation, antibacterial efficiency is obviously increased.

ACKNOWLEDGMENTS

We appreciate the financial support by the Scientific Research Projects Commission of Sakarya University (Project number: 2016-02-04-047).

REFERENCES

- [1] P. Guo, G. Zhang, J. Yu, H. Li, X.S. Zhao, "Controlled synthesis, magnetic and photocatalytic properties of hollow spheres and colloidal nanocrystal clusters of manganese ferrite," *Colloids and Surfaces A: Physicochemical and Engineering Aspects*, vol. 395, pp. 168–174, 2012.
- [2] G. Tong, F. Du, W. Wu, R. Wu, F. Liu, Y. Liang, "Enhanced reactive oxygen species (ROS) yields and antibacterial activity of spongy ZnO/ZnFe₂O₄ hybrid micro-hexahedra selectively synthesized through a versatile glucose-engineered co-precipitation/annealing process," *Journal of Materials Chemistry B*, vol. 1, pp. 2647–2657, 2013.
- [3] R. Liu, M. Lv, Q. Wang, H. Li, P. Guo, X.S. Zhao, "Solvothermal synthesis of size-tunable ZnFe₂O₄ colloidal nanocrystal assemblies and their electrocatalytic activity towards hydrogen peroxide," *Journal of Magnetism and Magnetic Materials*, vol. 424, pp. 155–160, 2017.
- [4] P. Guo, M. Lv, G. Han, C. Wen, Q. Wang, H. Li, X.S. Zhao, "Solvothermal synthesis of hierarchical colloidal nanocrystal assemblies of ZnFe₂O₄ and their application in water treatment," *Materials*, vol. 9, no. 806, pp. 1–10, 2016.
- [5] R. Ji, C. Cao, Z. Chen, H. Zhai, J. Bai, "Solvothermal synthesis of Co_xFe_{3-x}O₄ spheres and their microwave absorption properties," *Journal of Materials Chemistry C*, vol. 2, pp. 5944–5954, 2014.
- [6] N. Sanpo, C.C. Berndt, J. Wang, "Microstructural and antibacterial properties of zinc-substituted cobalt ferrite nanopowders synthesized by sol-gel methods," *Journal of Applied Physics*, vol. 112, pp. 1–7, 2012.
- [7] N. Sanpo, C. Wen, C.C. Berndt, J. Wang, "Antibacterial properties of spinel ferrite nanoparticles, in: Microbial Pathogens and Strategies for Combating Them," *Science, Technology and Education* (A. Méndez-Vilas, Ed.), pp. 239–250, 2013.
- [8] X. Hu, L. Xiao, X. Jian, W. Zhou, "Synthesis of mesoporous silica-embedded TiO₂ loaded with Ag nanoparticles for photocatalytic hydrogen evolution from water splitting," *Journal of Wuhan University of Technology- Materials Science Edition*, vol. 32, pp. 67–75, 2017.
- [9] Y. Chen, Y. Deng, Y. Pu, B. Tang, Y. Su, J. Tang, "One pot preparation of silver nanoparticles decorated TiO₂ mesoporous microspheres with enhanced antibacterial activity," *Materials Science and Engineering C*, vol. 65, pp. 27–32, 2016.
- [10] M. Rai, A. Yadav, A. Gade, "Silver nanoparticles as a new generation of antimicrobials," *Biotechnology Advances*, vol. 27, pp. 76–83, 2009.
- [11] S.W. Chook, C.H. Chia, S. Zakaria, M.K. Ayob, K.L. Chee, N.M. Huang, H.M. Neoh, H.N. Lim, R. Jamal, R. Rahman, "Antibacterial performance of Ag nanoparticles and AgGO nanocomposites prepared via rapid microwave-assisted synthesis method," *Nanoscale Research Letters*, vol. 7, pp. 1–7, 2012.
- [12] R. Verma, V.B. Chaudhary, L. Nain, A.K. Srivastava, "Antibacterial characteristics of TiO₂ nano-objects and their interaction with biofilm," *Materials Technology*, vol. 32, pp. 385–390, 2017.
- [13] C.M.N. Chan, A.M.C. Ng, M.K. Fung, H.S. Cheng, M.Y. Guo, A.B. Djurišić, F.C.C. Leung, W.K. Chan, "Antibacterial and photocatalytic activities of TiO₂ nanotubes," *Journal of Experimental Nanoscience*, vol. 8, pp. 859–867, 2013.
- [14] C. Cao, J. Huang, L. Li, C. Zhao, J. Yao, "Highly dispersed Ag/TiO₂ via adsorptive self-assembly for bactericidal application," *RSC Advances*, vol. 7, pp. 13347–13352, 2017.
- [15] J. Zhang, X. Liu, X. Suo, P. Li, B. Liu, H. Shi, "Facile synthesis of Ag/AgCl/TiO₂ plasmonic photocatalyst with efficiently antibacterial activity," *Materials Letters*, vol. 198, pp. 164–167, 2017.
- [16] W. Gu, Q. Xie, C. Qi, L. Zhao, D. Wu, "Phosphate removal using zinc ferrite synthesized through a facile solvothermal technique," *Powder Technology*, vol. 301, pp. 723–729, 2016.
- [17] S. Çakar, M. Özacar, "The effect of iron complexes of quercetin on dye-sensitized solar cell efficiency," *Journal of Photochemistry & Photobiology, A: Chemistry*, vol. 346, pp. 512–522, 2017.
- [18] N. Güy, M. Özacar, "The influence of noble metals on photocatalytic activity of ZnO for Congo red degradation," *International Journal of*

- Hydrogen Energy*, vol. 41, pp. 20100–20112, 2016.
- [19] X. Chen, Y. Dai, T. Liu, J. Guo, X. Wang, F. Li, "Magnetic core-shell carbon microspheres (CMSs)@ZnFe₂O₄/Ag₃PO₄ composite with enhanced photocatalytic activity and stability under visible light irradiation," *Journal of Molecular Catalysis A: Chemical*, vol. 409, pp. 198–206, 2015.
- [20] R. Liu, H. Ge, X. Wang, J. Luo, Z. Li, X. Liu, "Three-dimensional Ag-tannic acid-graphene as an antibacterial material," *New Journal of Chemistry*, vol. 40, pp. 6332–6339, 2016.
- [21] Z. Yang, Y. Wan, G. Xiong, D. Li, Q. Li, C. Ma, R. Guo, H. Luo, "Facile synthesis of ZnFe₂O₄/reduced graphene oxide nanohybrids for enhanced microwave absorption properties," *Materials Research Bulletin*, vol. 61, pp. 292–297, 2015.
- [22] L. Zhang, C. Ni, H. Jiu, C. Xie, J. Yan, G. Qi, "One-pot synthesis of Ag-TiO₂/reduced graphene oxide nanocomposite for high performance of adsorption and photocatalysis," *Ceramics International*, vol. 43, pp. 5450–5456, 2017.
- [23] R. Rahimi, M. Heidari-Golafzani, M. Rabbani, "Preparation and photocatalytic application of ZnFe₂O₄@ZnO core-shell nanostructures," *Superlattices and Microstructures*, vol. 85, pp. 497–503, 2015.
- [24] G. J. Rani, M. A. J. Rajan, "Reduced graphene oxide/ZnFe₂O₄ nanocomposite as an efficient catalyst for the photocatalytic degradation of methylene blue dye," *Research on Chemical Intermediates*, vol. 43, pp. 2669–2690, 2017.
- [25] J. Shen, G. Ma, J. Zhang, W. Quan, L. Li, "Facile fabrication of magnetic reduced graphene oxide-ZnFe₂O₄ composites with enhanced adsorption and photocatalytic activity," *Applied Surface Science*, vol. 359, pp. 455–468, 2015.
- [26] Y. Zhao, Z. Huang, W. Chang, C. Wei, X. Feng, L. Ma, X. Qi, Z. Li, "Microwave-assisted solvothermal synthesis of hierarchical TiO₂ microspheres for efficient electro-field-assisted-photocatalytic removal of tributyltin in tannery wastewater," *Chemosphere*, vol. 179, pp. 75–83, 2017.
- [27] J. S. Kim, E. Kuk, K. N. Yu, J. H. Kim, S. J. Park, H. J. Lee, S. H. Kim, Y. K. Park, Y. H. Park, C. Y. Hwang, Y. K. Kim, Y. S. Lee, D. H. Jeong, M. H. Cho, "Antimicrobial effects of silver nanoparticles," *Nanomedicine: Nanotechnology, Biology, and Medicine*, vol. 3, pp. 95–101, 2007.
- [28] Y. Z. Wang, Y. S. Wu, X. X. Xue, H. Yang, Z. H. Liu, "Microstructure and antibacterial activity of ions (Ce, Y, or B)-doped Zn-TiO₂: a comparative study," *Materials Technology*, vol. 32, pp. 310–320, 2017.
- [29] A. Allafchian, S. A. H. Jalali, H. Bahramian, H. Ahmadvand, "Preparation, characterization, and antibacterial activity of NiFe₂O₄/PAMA/Ag-TiO₂ nanocomposite," *Journal of Magnetism and Magnetic Materials*, vol. 404, pp. 14–20, 2016.
- [30] K. Atacan, M. Özacar, M. Özacar, "Investigation of antibacterial properties of novel papain immobilized on tannic acid modified Ag/CuFe₂O₄ magnetic nanoparticles," *International Journal of Biological Macromolecules*, vol. 109, pp. 720–731, 2018.